Enhanced major histocompatibility complex class I binding and immune responses through anchor modification of the non-canonical tumour-associated mucin 1-8 peptide

Eliada Lazoura,[1] Jodie Lodding,[1] William Farrugia,[2] Paul A. Ramsland,[2] James Stevens,[3] Ian A. Wilson,[3,4] Geoffrey A. Pietersz[5] and Vasso Apostolopoulos[1]

[1]*Burnet Institute at Austin, Immunology and Vaccine Laboratory, Heidelberg, VIC, Australia,* [2]*Burnet Institute at Austin, Structural Immunology Laboratory, Heidelberg, VIC, Australia,* [3]*Department of Molecular Biology, The Scripps Research Institute, La Jolla, CA, USA,* [4]*Skaggs Institute for Chemical Biology, The Scripps Research Institute, La Jolla, CA, USA, and* [5]*Burnet Institute at Austin, Bio-Organic and Medicinal Chemistry Laboratory, Heidelberg VIC Australia*

doi:10.1111/j.1365-2567.2006.02434.x
Received 19 February 2006; revised 20 June 2006; accepted 20 June 2006.
Correspondence: Professor Vasso Apostolopoulos and Dr Eliada Lazoura, Burnet Institute at Austin, Kronheimer Building, Studley Road, Heidelberg, VIC 3084 Australia.
Email: vasso@burnet.edu.au; eliadalazoura@hotmail.com
Senior author: Professor Vasso Apostolopoulos

Summary

Designing peptide-based vaccines for therapeutic applications in cancer immunotherapy requires detailed knowledge of the interactions between the antigenic peptide and major histocompatibility complex (MHC) in addition to that between the peptide–MHC complex and the T-cell receptor. Past efforts to immunize with high-affinity tumour-associated antigenic peptides have not been very immunogenic, which may be attributed to the lack of T cells to these peptides, having been deleted during thymic development. For this reason, low-to-medium affinity non-canonical peptides represent more suitable candidates. However, in addition to the difficulty in identifying such antigens, peptide binding to MHC, and hence its ability to induce a strong immune response, is limited. Therefore, to enhance binding to MHC and improve immune responses, anchor modifications of non-canonical tumour-associated peptides would be advantageous. In this study, the non-canonical tumour-associated peptide from MUC1, MUC1-8 (SAPDTRPA), was modified at the MHC anchor residues to SAPDFRPL (MUC1-8-5F8L) and showed enhanced binding to H-2K^b and improved immune responses. Furthermore, the crystal structure of MUC1-8-5F8L in complex with H-2K^b was determined and it revealed that binding of the peptide to MHC is similar to that of the canonical peptide OVA8 (SIINFEKL).

Keywords: anchor modifications; H-2K^b; mucin 1; non-canonical peptide; mucin 1-8; vaccine design

Introduction

Immunization with peptides derived from tumour antigens was successful in experimental mouse models with the induction of cytotoxic T lymphocytes (CTL) and tumour protection.[1] The efficacy of the immunization depends on the ability of peptides to induce and activate high-avidity CTL. High-affinity peptides from non-self antigens that bind to major histocompatibility complex (MHC) class I molecules usually induce such high-avidity CTLs. However, if the peptide is derived from a tumour antigen, vaccination may not be effective. MUC1, like most other tumour antigens, is expressed in normal tissues and overexpressed on cancer cells [termed tumour-associated antigens (TAA)]. Since most tumour antigens are self antigens, their specific CTL repertoire would most likely be deleted, as demonstrated for p53,[2–6] leading to tolerance. This tolerance is particularly associated with the high-affinity MHC-associated immunodominant epitopes, but not with low-affinity epitopes.[7] Thus, for tumour immunotherapy, it is conceivable that the best candidate peptides for immunization are low-affinity peptides.[8–18] However, peptide affinity and stability of the peptide–MHC complex have been shown

Abbreviations: APC, antigen-presenting cell; APL, altered peptide ligand; CTL, cytotoxic T lymphocytes; DC, dendritic cell; HLA, human leucocyte antigen; IFN-γ, interferon-γ; MHC, major histocompatibility complex; MPD, 2-methyl-2,4-pentanediol; MUC1, mucin 1; MWCO, molecular weight cut-off; pMHC, peptide-MHC; RMSD, root mean squared deviation; SFU, spot-forming units; TAA, tumour-associated antigen; TCR, T-cell receptor.

to correlate with overall immunogenicity.[19,20] Thus, a major problem in using low-affinity peptide epitopes for immunotherapy is the difficulty of their identification. Because such low-affinity peptides cannot be detected by elution studies and prediction algorithms, the only effective method for their identification is by systematic binding studies and recognition of peptide–MHC (pMHC) complexes by T-cell receptor (TCR). Therefore, it would be desirable to enhance the immunogenicity of low-affinity MHC-binding peptides by mutations of the peptide anchor side chains to increase their affinity.

The MHC class I molecule comprises a polymorphic glycosylated heavy chain (extracellular α1, α2 and α3 domains and short hydrophilic cytoplasmic tail) which is non-covalently associated with β_2-microglobulin. The α1 and α2 domains combine to form the peptide-binding groove of MHC. Understanding the mode of peptide binding to MHC class I molecules, with subsequent binding of the pMHC complex to the TCR, is a prerequisite to effective peptide vaccine design. Presently, canonical consensus sequences dominate the selection process.[19,21–23]

Numerous X-ray crystallographic studies have shown how a number of different high-affinity eight- or nine-mer peptides bind to the mouse MHC class I molecule, H-2K^b, and despite differences in the primary structure of these peptides, they all bound with similar conformations.[24–26] It is well documented that peptides that bind to H-2K^b require the amino acids, F/Y at position 5 (P5) and M/V/L at P8 for eight-mer peptides; P5 generally binds in the 'C' pocket and P8 binds in the 'F' pocket. However, it is now recognized that peptides with non-canonical anchors can bind to H-2K^b and still induce T-cell responses.[8,9,14,27,28] Indeed, the X-ray crystal structure of the low-affinity non-canonical anchor motif-containing peptide, MUC1-8 (SAPDTRPA), derived from mucin 1 (MUC1),[14] contained the small polar amino acid Thr at P5 and small non-polar Ala at P8 and bound in the C and F pockets, respectively.[14] The backbone structure of the low-affinity peptide, MUC1-8, bound similarly to high-affinity peptides, except, the C and F pockets were not completely filled, resulting in large cavities. We recently demonstrated that modifying the central Thr amino acid to Thr-GalNAc increased the affinity of the peptide and the GalNAc residue enabled high-affinity binding and generated high avidity T-cell responses.[16]

Herein, mutations to the MUC1-8 peptide were introduced at either or both, the central (P5) or C-terminal (P8) anchor residues, to increase the binding affinity to H-2K^b. Specifically, MUC1-8-5F (substituting Thr-P5 to Phe), MUC1-8-8L (substituting the Ala-P8 to Leu) and MUC1-8-5F8L (substitutions of Thr-P5 to Phe and Ala P8 to Leu) anchor-modified peptides were tested. In this study, we determined the X-ray crystal structure of MUC1-8-5F8L peptide in complex with H-2K^b at a resolution of 2·7 Å. The structure was compared to that of the non-canonical parent peptide MUC1-8 and the canonical OVA8 peptide (SIINFEKL). In addition, by molecular modelling we predicted the structures of MUC1-8-5F and MUC1-8-8L. MUC1-8-5F8L peptide displayed the highest affinity for H-2K^b and was more immunogenic in MUC1 × HLA-A2 transgenic mice; MUC1-8 in these mice was weakly immunogenic.

Materials and methods

Peptides

Peptides, SAPDTRPA (MUC1-8) the anchor modified analogues SAPD**F**RPA (MUC1-8-5F), SAPDTRP**L** (MUC1-8-8L) and SAPD**F**RP**L** (MUC1-8-5F8L) were synthesized. The high-affinity binding peptides, SIINFEKL – chicken ovalbumin$_{257–264}$ (OVA8), FAPGNYPAL – Sendai virus NP$_{324–332}$ (SEV9) and RGYVYQGL – vesicular stomatitis virus NP$_{52–59}$ (VSV8) were used in this study to compare to MUC1-8 anchor-modified peptides. All peptides were synthesized by Chiron Mimotopes (Clayton, VIC, Australia); the purity was >95% and molecular weights were confirmed by electrospray mass spectroscopy.

Production of soluble H-2K^b

The soluble extracellular domains of H-2K^b (heavy-chain residues 1–274 with C-terminal His-tag and β_2-microglobulin residues 1–99) were expressed in *Drosophila melanogaster* cells, under the control of a metallothione promoter as previously described.[25,29–31] Briefly, *D. melanogaster* cells were expanded to a large scale (up to 6 l) in serum free Insect Xpress® media (Cambrex, East Rutherford, NJ) and $CuSO_4$ (625 μM final concentration) was added 3–5 days before harvesting to induce expression of H-2K^b. The supernatant was concentrated using a CENTRAMATE tangential flow concentrator (PALL, East Hills, NY) using a 10 000 MWCO membrane (PALL) and then loaded onto a nickel-nitrilotriacetic acid (Ni-NTA) column and eluted using 10–250 mM imidazole buffer gradient, pH 7·5. Further purification was achieved using a Mono-Q column (GE Healthcare, Piscaloway, NJ; elution using 25–500 mM NaCl gradient, in a Tris–HCl buffer, pH 8·0) and the final sample was dialysed overnight against double-distilled water. This was further concentrated using a Nanosep 10 000 MWCO concentrator (PALL) to achieve final concentrations of 10–15 mg/ml, which were checked using the NanoDrop spectrophotometer (NanoDrop Technologies, Wilmington, DE).

Affinity measurements

Affinity measurements for binding of peptides to soluble H-2K^b molecules were performed as previously

described.[30,32] All affinity measurements were repeated at least two or three times.

Peptide stabilization assay using RMA-S cells

MHC class I molecules in the murine cell line RMA-S (C57BL/6 TAP2-deficient cells) can be used to measure the direct binding of peptides to class I molecules *in vitro*. RMA-S cells (5×10^5 cells) were incubated with peptides (10^{-4} to 10^{-13} M) at 26° for 3 hr then transferred to 37° for 30 min. After washing with 0·5% bovine serum albumin/phosphate-buffered saline (2 ml), anti-H-2K^b (HB-158) immunoglobulin G2a as supernatant (1/50 dilution, 100 μl) was added to RMA-S peptide-loaded cells and incubated for 45 min at 4°. The cells were washed once again and 100 μl (1/500 dilution) of fluorescein isothiocyanate-conjugated sheep $(Fab')_2$ anti-mouse immunoglobulin was added and incubated for 45 min at 4°; after further washing, cells were analysed by FACScan.

Mice, generation of dendritic cells (DC) and immunizations

C57BL/6 (H-2^b) or MUC1 × HLA-A2 (H-2^b/H-2^d/HLA-A2) transgenic 6- to 8-week-old mice were used in the experiments. Bone marrow cells from C57BL/6 or MUC1 × HLA-A2 female mice were cultured at 1×10^6 cells/ml in tissue culture media, supplemented with 10 ng/ml granulocyte–macrophage colony-stimulating factor/interleukin-4. At day 6, cells were washed, re-suspended in the same culture medium and 20 μg/ml peptides were loaded on DCs for 3 hr. Pulsed DC were washed and 100 μl (1×10^6–2×10^6 cells) was injected intradermally in female mice into the base of tail. After 14 days mice were boosted and 16 days later splenocytes were assessed by ELISpot. All animal studies were approved by the Austin Health ethics committee.

ELISpot assay

To assess peptide specific interferon-γ (IFN-γ) production by CD8$^+$ T cells to each peptide, splenocytes from immunized mice were used in IFN-γ ELISpot assays. Spleen cells were incubated with 10^{-5} to 10^{-10} M of each MUC1 peptide, irrelevant peptide (OVA8, SIINFEKL) or internal positive control concanavalin A for 18 hr at 37°, 8% CO_2 on nitrocellulose plates (precoated with an anti-murine IFN-γ monoclonal antibody). Plates were developed as previously described.[33–35]

Preparation and crystallization of the H-2K^b/MUC1-8-5F8L complex

The soluble extracellular domains of H-2K^b (heavy chain residues 1–274 and β_2-microglobulin residues 1–99) were expressed in *Drosophila melanogaster* cells, as previously described.[25,29–31] Large crystals of the H-2K^b-MUC1-8-5F8L complex (> 10 mg/ml) grew in 1·8–2·0 M NaH_2PO_4/K_2HPO_4 with 1–2% (v/v) 2-methyl-2,4-pentanediol (MPD), pH 6·6–7·4, at 18° with fivefold molar excess of MUC1-8-5F8L peptide. H-2K^b and peptide were both in double-distilled water (preincubated overnight at 4° before crystal set up), and crystals were set up using the sitting drop vapour diffusion method, with 0·5 μl MHC–peptide mixture applied to the platform immediately followed by the addition of 0·5 μl of mother liquor. One millilitre of mother liquor was added to each well of a 24-well Cryschem plate (Hampton Research, Aliso Viejo, CA). Crystals appeared within 5 days and grew to dimensions of 0·2 × 0·2 × 0·1 mm within 2 weeks.

Data collection and structure determination

Before data collection, crystals were harvested in a NaH_2PO_4/K_2HPO_4 solution, 0·2 M lower than that in which the crystals were grown, 1–2% MPD, pH 6·6–7·4 and 25% (v/v) glycerol as cryoprotectant. Crystals were cryocooled to − 170° in a nitrogen gas stream. X-ray diffraction data were collected using a MicroMax007 Rigaku X-ray generator (Rigaku, Tokyo, Japan) operated at 40 kV and 20 mA. X-rays were focused to 0·3-mm diameter using Osmic Blue confocal optics and diffraction images ($\Delta\varphi = 0{\cdot}5°$) were captured on an R-Axis IV^{++} detector at a crystal-to-detector distance of 200 mm. Diffraction data were processed using the HKL program suite version 1.96.6.[36] Relevant data-processing statistics are presented in Table 1.

The H-2K^b-MUC1-8-5F8L crystals belong to the orthorhombic $P2_12_12$ space group, as do the MUC1-8, OVA8, VSV8, SEV9 and YEA9-H-2K^b complexes.[13,14,25,26] The structure was determined by phasing the data using the co-ordinates of the high resolution (1·6 Å) H-2K^b-MUC1-8 structure (PDB 1G7Q[14]) using the CNS program. The MUC1-8 peptide was initially removed and the MUC1-8-5F8L peptide was built into the $|F_o| - |F_c|$ electron density using the program TURBO-FRODO version 5·5 (BioGraphics, Marseille, France).[37]

Cross-validated crystallographic refinements against maximum likelihood targets were carried out with the CNS program suite, version 0·9.[38] Between cycles of crystallographic refinement, the model was fitted to $2|F_o| - |F_c|$ and $|F_o| - |F_c|$ maps on a Silicon Graphics workstation, using the program TURBO-FRODO.[37] The carbohydrate moieties (NAG and FUC), PO_4^{3-} ions and solvent (MPD and water) were added to the model when the crystallographic *R*-factor (R_{work}) dropped below 0·25. A bulk solvent correction and anisotropic overall *B*-factor refinements were applied during the last cycles of the structure refinement. Table 2 summarizes the last stage of refinement and the quality of the model as assessed by PROCHECK.[39] Analysis of the final model

Table 1. Crystallographic data collection and refinement statistics

Space group	$P2_12_12$
Cell dimensions (Å)	$a = 135{\cdot}26$, $b = 87{\cdot}89$, $c = 45{\cdot}16$
Resolution range (Å)	50·0–2·7 (2·8–2·7)
R_{merge} (%)	10·4 (43·4)
No. of reflections	14 383
Data completeness (%)	97·9 (96·2)
Data redundancy	6·4 (5·3)
$<I/\sigma(I)>$	17·4 (3·3)
R_{work} (%)	19·3
R_{free} (%)	24·7
RMSD from ideal values	
Bond length (Å)	0·006
Bond angle (°)	1·4
Dihedral angle (°)	24·7
Improper angle (°)	0·79
B-values from Wilson plot (Å^2) (Mean)	54·4 (37·5)
No. residues	
Protein	373
Peptide	8
No. solvent molecules	
H_2O	104
PO_4^{3-}	2
MPD	4
Ramachandran plot values (%)	
Most-favoured regions	89·3
Additionally allowed regions	9·8
Generously allowed regions	0·9
Disallowed regions	0·0

Table 2. Affinity measurements of peptides binding to H-2K^b

Peptide	Sequence	K_D 4° (nM)	K_D 23° (nM)	K_D 37° (nM)
MUC1-8	SAPDTRPA	433	877	37 000
MUC1-8-5F	SAPDFRPA	460	130	4900
MUC1-8-8L	SAPDTRPL	150	250	8900
MUC1-8-5F8L	SAPDFRPL	160	60	300
OVA8	SIINFEKL	6	10	82
VSV8	RGYVYQGL	34	27	163
SEV9	FAPGNYPAL	5	3	30

The affinity values in this table are the means of five values.[14]
The standard errors of these values are between 10 and 15%.

with PROCHECK[39] showed 89·3% of the residues are in the most favoured regions of the Ramachandran plot, with none in the disallowed regions. The electron density for all residues was well-defined, except for the MHC polypeptide turn side chain regions. Figures were prepared using TURBO-FRODO 5·5 and DS MODELING 1·1 (Accelrys Inc., San Diego, CA).

Protein Data Bank accession codes

The atomic co-ordinates and structure factors for the H-2K^b–MUC1-8-5F8L complex have been deposited in the RCSB Protein Data Bank with accession code 2FO4.

Molecular modelling

Models of the MUC1-8 peptide analogues (MUC1-8-5F and MUC1-8-8L) were based on the MUC1-8-5F8L crystal structure of the α-chain of the mouse MHC class I molecule H-2K^b complexed to MUC1-8-5F8L (described herein). Molecular modelling was performed with the DS MODELING 1·1 software (Accelrys) using the CHARMm forcefield to optimize the molecular geometry. Before the molecular dynamics simulation, structures were relaxed using a steepest descent gradient algorithm until the root mean square deviation (RMSD) was less than 0·1 kcal/mol, then followed by the Adopted Basis-set Newton–Raphson algorithm until the RMSD was less than 0·01 kcal/mol. A distance dependent dielectric was used to simulate aqueous solvent conditions. Peptide molecules and all atoms within a 20-Å radius of the peptide were subsequently heated to room temperature (300 K) in 1000 steps and equilibrated at this temperature for a further 1000 steps before commencing the molecular dynamics run for 200 ps, storing the structure every 100 steps.

The final conformation was selected for all further analysis. The RMSD between the main-chain Cα atoms was calculated for all residues between MUC1-8, OVA8, MUC1-8-5F8L and the anchor-modified analogues (MUC1-8-5F and MUC1-8-8L) as a measure of variation in peptide conformation. All satisfied H-bonds and salt bridges between peptide and H-2K^b molecule were identified.

Results

Affinity measurements of MUC1-8 peptide mutants with soluble H-2K^b

As the MUC1-8 peptide did not contain any preferred anchor residues at P2, P5 and P8, it was found to bind with low affinity, but induced CTLs in C57BL/6 mice.[14] The affinity of MUC1-8 was measured in an inhibition assay to be $4{\cdot}3 \times 10^{-7}$ M at 4°, $8{\cdot}7 \times 10^{-7}$ M at 23° (100–300-fold lower than OVA8, or other high-affinity peptides VSV8 and SEV9; Table 2).[14] Mutation of Thr-P5 to Phe-P5 (MUC1-8-5F) increased peptide affinity by at least sevenfold at 23° and 37°, and mutation of Ala-P8 to Leu-P8 (MUC1-8-8L) increased affinity by at least threefold at 23° and 37°, whilst the double mutant of Thr-P5/Ala-P8 to Phe-P5/Leu-P8 (MUC1-8-5F8L) increased the affinity of the peptide significantly more than the single mutants, by 14-fold at 23°, and provided higher thermal stabilization at 37° (Table 2).[14]

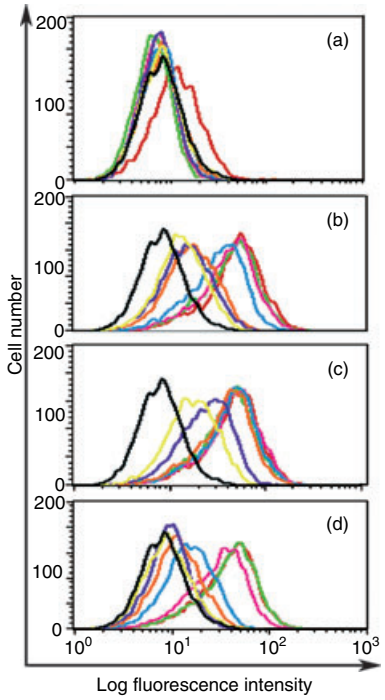

Figure 1. Stabilization of MHC class I molecule, H-2K^b. Flow cytometric analysis of RMA-S cells pulsed with (a) MUC1-8 (SAPDTRPA), (b) MUC1-8-5F (SAPDFRPA), (c) MUC1-8-5F8L (SAPDFRPL) and (d) MUC1-8-8L (SAPDTRPL), before incubation with anti-H-2K^b-specific antibody. Various peptide concentrations were added and labelled as: 10^{-4} M (red), 10^{-5} M (green), 10^{-6} M (pink), 10^{-7} M (light blue), 10^{-8} M (orange), 10^{-9} M (purple), 10^{-10} M (yellow), no peptide (black).

Stabilization of MHC class I on RMA-S cells with MUC1-8, MUC1-8-5F, MUC1-8-8L, MUC1-8-5F8L peptides

We determined the binding of MUC1-8, MUC1-8-5F, MUC1-8-8L, MUC1-8-5F8L peptides to MHC class I, H-2K^b, in assembly assays, based on peptide-dependent stabilization of MHC heavy chains in TAP2-deficient cells (RMA-S) at 26°. MUC1-8 stabilized MHC class I, H-2K^b, at $>10^{-4}$ M; MUC1-8-5F stabilized H-2K^b, at $>10^{-7}$ M; MUC1-8-8L stabilized H-2K^b at $>10^{-6}$ M and MUC1-8-5F8L stabilized H-2K^b at $>10^{-9}$ M (Fig. 1).

Generation of T cells *in vivo*

The *ex vivo* 18 hr ELISpot assay does not require cell expansion because it detects specifically activated memory effector cells (both CD4 and CD8 cytokine-producing terminal effectors). The sensitivity of the assay is higher than limiting dilution analysis, FACscan analysis or enzyme-linked immunosorbent assay, and can reliably detect the precursor frequencies of antigen-specific effectors of 1 in every 500 000 cells.[14,16,40–44] It is therefore an appropriate method to detect antigen-specific cells at low precursor frequencies as demonstrated previously in malaria models[40–44] and thus, we did not do CTL assays.

The ability of MUC1-8, MUC1-8-5F, MUC1-8-8L, MUC1-8-5F8L peptides to induce T-cell responses in C57BL/6 mice was measured using IFN-γ by ELISpot analysis after recognition of MUC1-8, MUC1-8-5F, MUC1-8-8L and MUC1-8-5F8L peptides at varying concentrations (10^{-5} to 10^{-12} M). Mice immunized with DC-MUC1-8 generated IFN-γ-secreting T cells which recognized all peptides at a concentration of 10^{-7} to 10^{-5} M (Fig. 2a.i). T cells from mice immunized with DC-MUC1-8-5F or MUC1-8-5F8L generated IFN-γ-secreting T cells which recognized all peptides in the range 10^{-10} to 10^{-5} M; however, the number of spot-forming units (SFU)/500 000 was higher in mice immunized with MUC1-8-5F8L (Fig. 2a.ii,iii). Mice immunized with MUC1-8-8L generated T cells that recognized all other peptides at 10^{-9} to 10^{-5} M (Fig. 2a.iv). Thus, the induction of T cells correlated with the affinity of the peptide, i.e. in increasing strength is, MUC1-8-5F8L > MUC1-8-5F > MUC1-8-8L > MUC1-8.

As it is clear that MUC1-8 is immunogenic in C57BL/6 mice it is not immunogenic in MUC1 × HLA-A2 transgenic mice (Fig. 2b.i). However, mutations to the MUC1-8 peptide to result in MUC1-8-5F, MUC1-8-5F8L and MUC1-8-8L increased the magnitude of T-cell responses in MUC1 × HLA-A2 transgenic mice (where MUC1-8 is self) (Fig. 2b); MUC1-8-5F and MUC1-8-8L recognized all peptides 10-fold higher than MUC1-8 (Fig. 2b.i,ii,iv) and mice immunized with the double mutant peptide analogue MUC1-8-5F8L generated even higher affinity T cells which recognized all peptides (Fig. 2b.iii). Furthermore, immunization of MUC1-8 peptide yielded a precursor frequency of 200 SFU/500 000 cells, i.e. 1/2500; immunization of MUC1-8-5F8L resulted in a precursor frequency of 400 SFU/500 000 cells, i.e. 1/1250. A twofold increase in precursor frequency can have dramatic effects on the protective efficacy of peptides *in vivo* and the recognition of tumour cells by CTL. We have demonstrated this for a range of MUC1 antigen formulations, where the precursor frequency correlated with tumour protection and CTL induction, and even a twofold increase gave dramatic effects.[45] In addition, our study and other studies of liver-stage malaria have shown a fourfold increase in protective efficacy of CD8 T cells upon a twofold increase in precursor frequency (from 1/8000 to 1/4000).[42] Importantly, the difference in these frequency values is statistically significant, indicating that MUC1-8-5F8L binds with higher affinity, providing quantitative functional data to corroborate the binding assay data demonstrated in Fig. 1 and Table 2. It is clear that, mutations to the native MUC1-8 peptide could overcome tolerance and result in generation of higher affinity T cells.

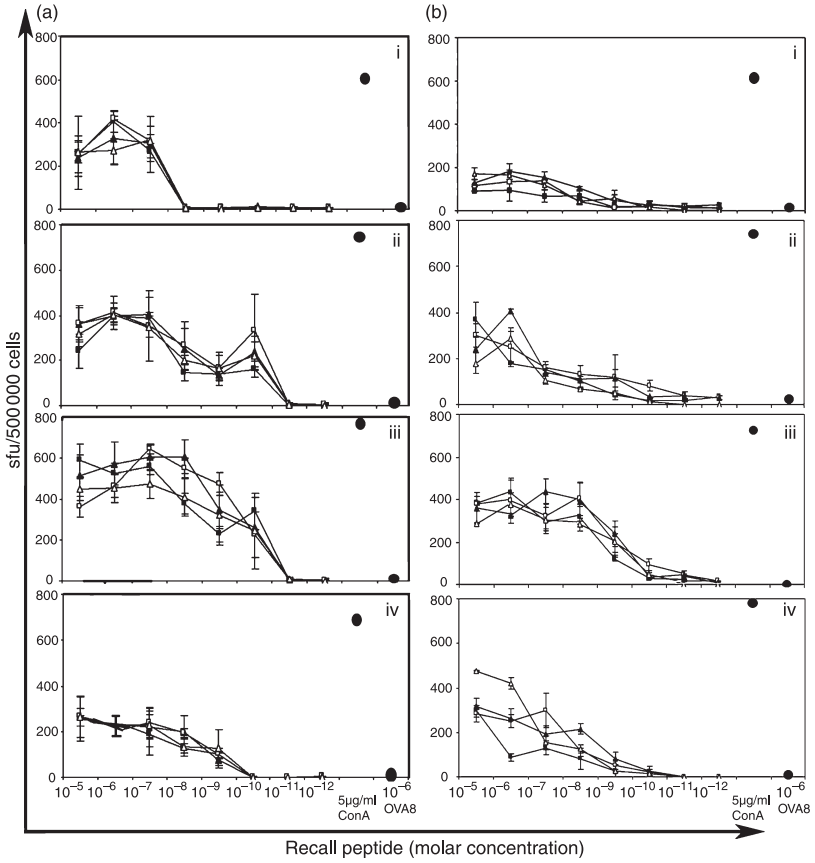

Figure 2. Measurement of IFN-γ secreted by T cells as measured by ELISpot assay. (a) C57BL/6 mice and (b) MUC1 × HLA-A2 transgenic mice were immunized with DC pulsed with (i) MUC1-8,(ii) MUC1-8-5F, (iii) MUC1-8-5F8L or (iv) MUC1-8-8L peptides. In all immunized mouse groups, specific IFN-γ-secreting CD8 T cells are generated which recognize MUC1-8 (■), MUC1-8-5F (□), MUC1-8-5F8L (▲) or MUC1-8-8L (△) peptides. OVA8 was used as a negative control and concanavalin A (non-specific stimulus of T cells) was used as an internal positive control. The data are presented as spot-forming units (SFU) per 5×10^5 cells. Experiments were performed at least twice with three mice/group.

Binding of MUC1-8-5F8L mutant peptide with H-2K^b – X-ray crystal structure

The crystal structure of H-2K^b–MUC1-8-5F8L at 2·7 Å resolution was determined by molecular replacement and refined to a final R_{work} of 19·3% and an R_{free} of 24·7% (Table 1). The final atomic co-ordinates consisted of H-2K^b heavy chain (residues 1–274), β_2-microglobulin (residues 1–99), four carbohydrate moieties (NAG at Asn^{86} and NAG and FUC at Asn^{176} of the heavy chain) and all peptide residues, P1–P8 (MUC1-8-5F8L). Additionally, two phosphate (PO_4^{3-}) and four MPD molecules were located. Electron density for the bound peptide was continuous and well resolved (Fig. 3a).

Superposition of MUC1-8-5F8L, MUC1-8 and OVA8 showed similar overlays when viewed from the side (Fig. 3b,c). The RMSD between MUC1-8 and MUC1-8-5F8L was very low (0·19 Å, Table 3), while that of OVA8 and MUC1-8-5F8L was considerably higher (0·57 Å, Table 3), but comparable with that between MUC1-8 and OVA8 (RMSD 0·51 Å; Fig. 3d).

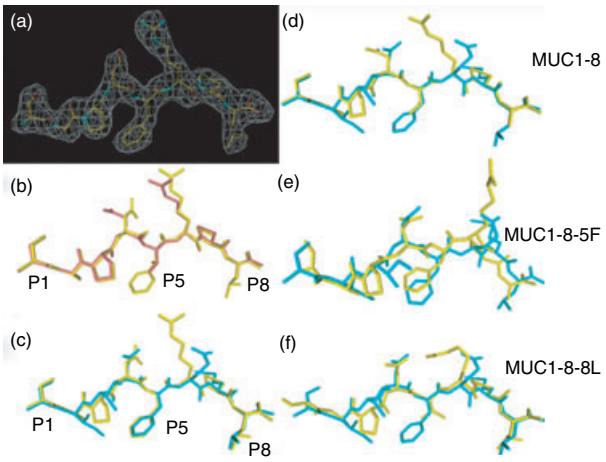

Figure 3. (a) Final electron density map of MUC1-8-5F8L. Cα backbone superimposition of (b) MUC1-8-5F8L and MUC1-8 and (c) MUC1-8-5F8L and OVA8. MUC1-8-5F8L is in yellow, MUC1-8 in pink and OVA8 in cyan. Cα backbone superimposition of OVA8 (cyan) with (d) MUC1-8 (crystal structure), (e) MUC1-8-5F (model) and (f) MUC1-8-8L (model). MUC1-8, MUC1-8-5F and MUC1-8-8L are in yellow.

Interactions of MUC1-8-5F8L peptide with H-2K^b – X-ray crystal structure

High-affinity interactions are consistent with the formation of a highly conserved hydrogen bond network between the side chains of the MHC and the peptide backbone, mainly around the N and C termini, and the optimal fit of peptide side chains into the MHC pockets.

Table 3. Cα backbone atom RMSD (Å)

	OVA8	MUC1-8	5F8L
OVA8			
MUC1-8	0·51		
5F8L	0·57	0·19	
5F	1·27	1·18	1·14
8L	0·60	0·58	0·55

Intermolecular H-bonds between peptide residues and MHC are summarized in Table 4 and Fig. 4. The number of water molecules located in the near vicinity of the peptide within the MHC groove varied between the crystal structures of MUC1-8-5F8L, MUC1-8 and OVA8. Fewer water molecules were found in the MUC1-8-5F8L crystal structure (six water molecules; Fig. 5a) than in the MUC1-8 crystal structure (10 water molecules; Fig. 5b), or in OVA8 (seven water molecules; Fig. 5b). The intermolecular salt bridges between Asp^{P4} with Arg^{155} and Arg^{P6} with Glu^{152} were conserved for the MUC1-8-5F8L crystal structure, despite the loss of the salt bridge between Asp^{P4} and Lys^{66} observed for MUC1-8. The intramolecular salt bridge observed between Asp^{P4} and Arg^{P6} was conserved in the MUC1-8-5F8L peptide, as was observed for the parent non-canonical peptide MUC1-8. For comparison, intermolecular salt bridges were observed between Arg^{155} with Glu^{P6} and Asp^{77} with Lys^{P7} for OVA8, with an intramolecular salt bridge also being present between Glu^{P6} and Lys^{P7}.

Peptide binding within the H-2K^b groove is predominantly attributed to the contribution of H-bonding and salt bridge formation. In addition, the involvement of water molecules, which assist with the binding of peptide residues to relevant residues within the H-2K^b pockets, namely C and F, is also a major contributing factor. Both C and F pockets of the H-2K^b–MUC1-8-5F8L crystal are occupied by the P5 and P8 side chains, similar to that observed for OVA8. The modification of the small P5 and P8 anchor residues of MUC1-8 to Phe and Leu, respectively, contributed to the strong binding of the MUC1-8-5F8L peptide to H-2K^b. In contrast, the weak binding of MUC1-8 to H-2K^b can be attributed to the lack of appropriate anchors at these positions to fill these pockets. As a result, the binding of peptide to MHC is via indirect H-bonding with water molecules in the vicinity of pockets C and F.

Interactions of MUC1-8 peptide analogues with H-2K^b – molecular modelling

The crystal structure of MUC1-8-5F8L was used to model the MUC1-8-5F and MUC1-8-8L peptide analogues. These resulting models were compared with the MUC1-8-5F8L crystal structure (described herein) as well as the parent non-canonical peptide MUC1-8 (1G7Q) and the canonical peptide OVA8 (1VAC) crystal structures. Comparisons were also made between MUC1-8-5F8L, MUC1-8 and OVA8 to assess the effect of anchor modification on binding to H-2K^b. RMSDs were calculated for the Cα backbone atoms and are listed in Table 3. Superimposition of MUC1-8-5F8L with the molecular models, MUC1-8-5F and MUC1-8-8L, yielded RMSD values of 1·18 Å and 0·58 Å, respectively. For comparison, all peptides were also superimposed with the canonical OVA8 peptide, which yielded RMSD values of 0·51 Å (MUC1-8), 0·57 Å (MUC1-8-5F8L), 0·60 Å (MUC1-8-8L) and 1·27 Å (MUC1-8-5F) (Fig. 3d–f). The largest deviation

Table 4. Intermolecular H-bonding between H-2K^b and peptides OVA8, MUC1-8, MUC1-8-5F8L (crystal structures) and MUC1-8-5F and MUC1-8-8L (models)

	OVA8	MUC1-8	MUC1-8-5F8L	MUC1-8-5F	MUC1-8-8L
P1	$S^{P1}O\gamma{:}K^{66}N\zeta$	$S^{P1}O\gamma{:}K^{66}N\zeta$	$S^{P1}O\gamma{:}K^{66}N\zeta$	$S^{P1}O\gamma{:}K^{66}N\zeta$	$S^{P1}O\gamma{:}K^{66}N\zeta$
	$S^{P1}O{:}Y^{159}OH$	$S^{P1}O{:}Y^{159}OH$			
	$S^{P1}N{:}Y^{171}OH$	$S^{P1}N{:}Y^{171}OH$			
	$S^{P1}N{:}Y^{7}OH$	$S^{P1}N{:}Y^{7}OH$			
	$S^{P1}O\gamma{:}E^{63}O\varepsilon2$	$S^{P1}O\gamma{:}E^{63}O\varepsilon2$			
P2	$I^{P2}O{:}K^{66}N\zeta$	$A^{P2}O{:}K^{66}N\zeta$	$A^{P2}O{:}K^{66}N\zeta$	$A^{P2}O{:}K^{66}N\zeta$	$A^{P2}O{:}K^{66}N\zeta$
P3	$I^{P3}O{:}N^{70}N\delta2$	$P^{P3}O{:}N^{70}N\delta2$	$P^{P3}O{:}N^{70}N\delta2$	$P^{P3}O{:}N^{70}N\delta2$	$P^{P3}O{:}N^{70}N\delta2$
P4	$N^{P4}O{:}R^{155}NH1$	$D^{P4}O{:}R^{155}NH1$	$D^{P4}O{:}R^{155}NH1$	$D^{P4}O{:}R^{155}NH1$	$D^{P4}O{:}R^{155}NH1$
	$N^{P4}O{:}R^{155}NH2$	$D^{P4}O{:}R^{155}NH2$	$D^{P4}O{:}R^{155}NH2$	$D^{P4}O{:}R^{155}NH2$	$D^{P4}O{:}R^{155}NH2$
	$N^{P4}O\delta1{:}R^{155}NH1$				
P5	$F^{P5}N{:}N^{70}O\delta1$	$T^{P5}N{:}N^{70}O\delta1$	$F^{P5}N{:}N^{70}O\delta1$	$F^{P5}N{:}N^{70}O\delta1$	$T^{P5}N{:}N^{70}O\delta1$
P6					
P7	$K^{P7}N\zeta{:}S^{73}O\gamma$	$P^{P7}O{:}W^{147}N\varepsilon1$	$P^{P7}O{:}W^{147}N\varepsilon1$	$P^{P7}O{:}W^{147}N\varepsilon1$	$P^{P7}O{:}W^{147}N\varepsilon1$
P8	$L^{P8}N{:}D^{77}O\delta1$	$A^{P8}N{:}D^{77}O\delta1$	$\mathbf{L}^{P8}N{:}D^{77}O\delta1$	$A^{P8}N{:}D^{77}O\delta1$	$\mathbf{L}^{P8}N{:}D^{77}O\delta1$
		$A^{P8}N{:}K^{146}N\zeta$	$\mathbf{L}^{P8}O{:}K^{146}N\zeta$	$A^{P8}O{:}K^{146}N\zeta$	$\mathbf{L}^{P8}O{:}K^{146}N\zeta$

Anchor modified residues in bold for peptide MUC1-8-5F8L (crystal structure), MUC1-8-5F and MUC1-8-8L (models).

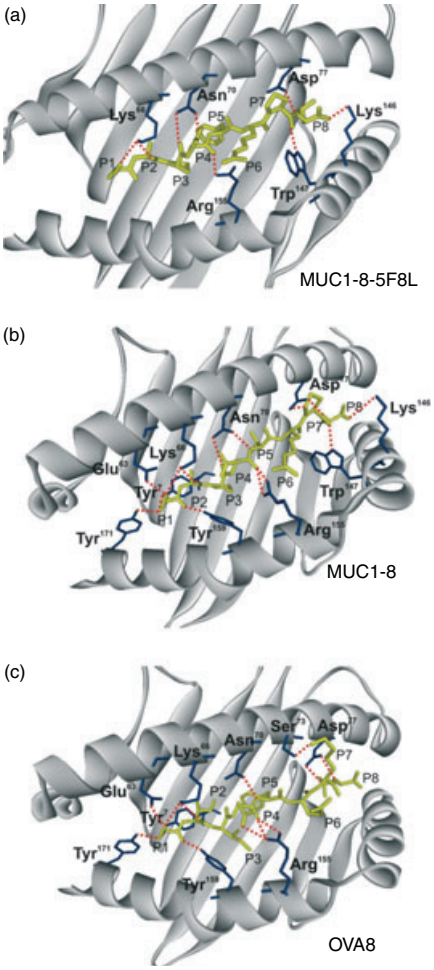

Figure 4. Hydrogen bond network within the H-2K^b binding groove for the crystal complexes with (a) MUC1-8-5F8L, (b) MUC1-8 and (c) OVA8. Residues from the peptide are labelled P1-P8 while those from the H-2K^b molecules are labelled with the amino acid three-letter code and numerical superscripts with dashed lines for H-bonds. Only the binding groove and peptide are shown.

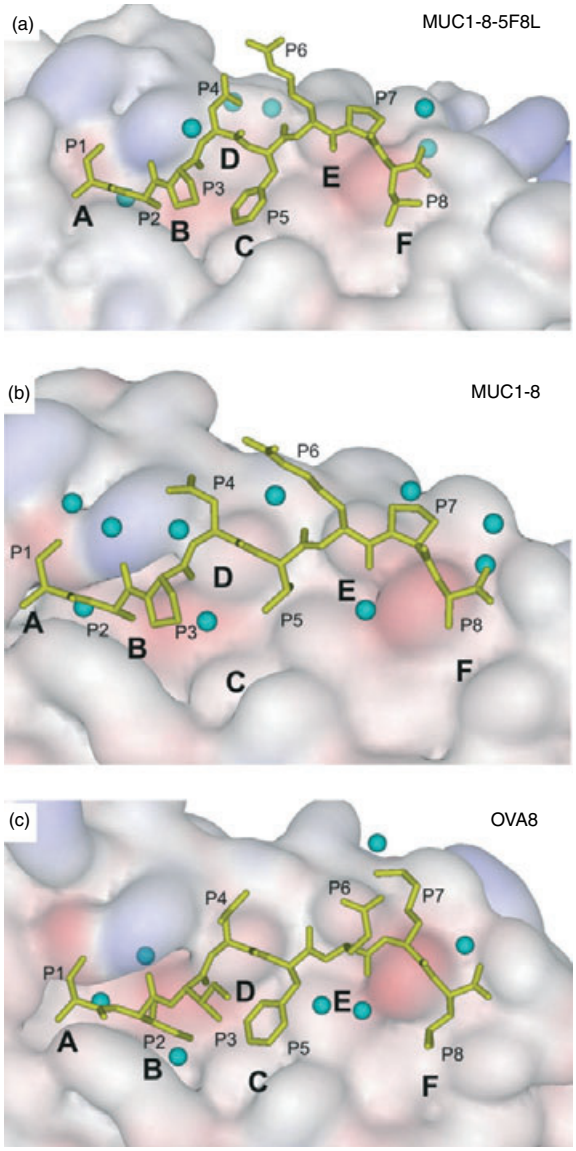

Figure 5. Location of water molecules (cyan spheres) within the binding groove of H-2K^b for (a) MUC1-8-5F8L, (b) MUC1-8 and (c) OVA8. Residues from the peptide are labelled P1-P8. The binding groove pockets are also indicated. Note how canonical anchor residues almost completely fill out the C and F pockets while the small non-canonical anchors leave these pockets largely unoccupied.

was observed between the 5F anchor modified peptide (MUC1-8-5F) with RMSD values of 1·27 Å (with OVA8), 1·18 Å (with MUC1-8) and 1·14 Å (with MUC1-8-5F8L). This data correlated well with the affinity measurements performed at 4° (Table 1). Intermolecular H-bonds (summarized in Table 4).

Discussion

The selection of suitable antigens to elicit an effective immunological response in cancer patients is the first step to designing an effective vaccine. However, tolerance to these antigens remains an obstacle to overcome. Furthermore, identification of the antigenic portion and most importantly the immunogenic fragments remains challenging. To date, medium-to-high affinity peptides selected for cancer immunotherapy have resulted in only limited success in clinical trials. For example, partial or complete tumour regression was observed in only 10–30% of patients receiving melanoma peptides.[46] The efficacy of high-affinity 'self' epitope to induce an effective CTL response and provide protection and eradication of tumour cells has been unsuccessful because of the absence of T cells, which have been deleted during the development of the immune system.[2–6] More recently low-to-medium affinity peptides have been selected, which have yielded more promising results.[47] For example, high vaccination efficiency was observed for heteroclitic variants

of low-affinity epitopes from the naturally expressed murine telomerase reverse transcriptase (mTERT)[47] and mice immunized with the low-affinity p572 and p988 epitopes resulted in protection against tumour challenge.[47] In addition, the recent identification and validation of seven low-affinity epitopes from known HLA-A2.1-restricted melanoma-associated antigens that do not conform to the canonical anchor motif for this HLA molecule were reported. Anchor modifications to these epitopes led to improved HLA binding and improved capacity to stimulate T cells.[48]

Previously, we reported the crystal structure of the low-affinity non-canonical MUC1-8 peptide in complex with H-2K^b.[14] Furthermore, MUC1-8 was also shown to be capable of inducing immune responses in mice despite the low affinity for H-2K^b. Herein, we report the crystal structure of the MUC1-8-5F8L peptide in complex with H-2K^b, which provides insight into the enhanced binding of the parent MUC1-8 peptide to H-2K^b following modification of the non-canonical anchor residues to canonical ones (Thr^{P5} to Phe and Ala^{P8} to Leu), MUC1-8-5F8L. Enhanced T-cell responses were observed, which varied depending on which anchor was modified. The biological data revealed that modification of the central anchor P5 to Phe (MUC1-8-5F), increased peptide affinity (as measured by competition studies) by sevenfold compared to modification of the P8 residue to Leu (MUC1-8-8L) which only increased threefold compared to MUC1-8. In comparison, MUC1-8-5F8L showed a significant 14-fold increase in binding affinity. Similar results were also obtained for the stabilization studies using TAP2-deficient RMA-S cells as determined by FACScan.

T-cell responses *in vivo* also revealed that C57BL/6 mice immunized with the doubly substituted MUC1-8 peptide, MUC1-8-5F8L, recognized all other peptides (MUC1-8, MUC1-8-5F and MUC1-8-8L) more strongly. Although weaker T-cell responses were observed in MUC1 × HLA-A2 transgenic mice, the overall trend revealed that they are more immunogenic (tolerance could be overcome) with anchor substitutions to the non-canonical low-affinity MUC1-8 peptide. Enhanced immunogenicity and binding of non-immunogenic low affinity peptides to HLA-A2.1 has been achieved with a tyrosine substitution at the P1 position. Binding affinity can be increased 55-fold and/or stabilized for more than 2 hr compared to parent peptides. Most importantly, the variants could trigger CTL that also recognize the parent peptide.[49] Similarly, enhanced immune responses and binding to H-2K^b were observed when the low-affinity MUT1 peptide, a TAA isolated from 3LL Lewis lung carcinoma, was modified at the anchor positions P3, P5 and P8.[50] Furthermore, we have immunized mice with a higher affinity peptide (SAPDTRPA to SAPDT-GalNAc-RPA) where the affinity is similar to that for MUC1-8-5F8L. The T cells that are generated recognized the mutated higher affinity peptide more efficiently compared to the non-mutated, lower affinity peptide.[16]

The crystal structure of MUC1-8-5F8L revealed that a number of H-bonds were lost at the N-terminus, namely Ser^{P1} with Tyr^7, Glu^{63}, Tyr^{159} and Tyr^{171} when compared to both the crystal structures of MUC1-8 and OVA8 in complex with H-2K^b. Different C-terminal H-bonds were also noted (Pro^{P7} with Tyr^{147} not Ser^{73} as for OVA8) and Leu^{P8} with Lys^{146} (also observed for MUC1-8 with P8 residue Ala). The bound conformation of the MUC1-8-5F8L peptide was very similar to that of MUC1-8 main-chain and comparable to that of OVA8. Interestingly, the number of water molecules surrounding the MUC1-8-5F8L peptide was lower^6 than that for MUC1-8^{10} and more comparable to that of OVA8^7. The C and F pockets are fully occupied by the larger hydrophobic residues, Phe and Leu, and help to stabilize the peptide within the binding groove in a similar manner to OVA8, attributed to the strong binding affinity of this peptide for H-2K^b. The large cavities present at both the C and F pockets in the MUC1-8 structure are occupied with water molecules which help stabilize the low-affinity MUC1-8 peptide; these water molecules are absent in the high-affinity binding peptides MUC1-8-5F8L and OVA8. It is noteworthy, that compared to OVA8 and MUC1-8, there are no water molecules in the E pocket of H-2K^b for the H-2K^b–MUC1-8-5F8L crystal structure.

The molecular modelling studies suggested that MUC1-8-5F deviated by the greatest amount from the parent MUC1-8 peptide structure, OVA8 and MUC1-8-5F8L (Table 3). RMSDs between MUC1-8-8L and MUC1-8, OVA8 and MUC1-8-5F8L were lower (Table 3), suggesting that modifications in the C terminus of the peptide do not affect the peptide–H-2K^b complex structure to the same extent; the data correlated well with the affinity data obtained at 4°.

Overall, this study validated the finding that anchor modifications made to non-canonical tumour epitopes, such as MUC1-8, can significantly enhance binding to the MHC class I molecule H-2K^b and, in this case, also improve T-cell responses. The results are very encouraging and warrant continued efforts to identify low-affinity peptides that can subsequently be modified to yield analogues with high affinity for MHC and potent T-cell stimulatory activity.

Acknowledgements

This work was supported by an NH & MRC project grant 223310 (V.A.), and a National Institutes of Health grant CA58896 (J.S., I.A.W.). V.A. (223316) and P.A.R. (365209) are NH & MRC R. Douglas Wright Fellows. The authors would like to thank Professor Ian McKenzie for helpful discussions.

References

1 Pietersz GA, Apostolopoulos V, McKenzie IF. Generation of cellular immune responses to antigenic tumor peptides. *Cell Mol Life Sci* 2000; **57**:290–310.

2 Cibotti R, Kanellopoulos JM, Cabaniols JP, Halle-Panenko O, Kosmatopoulos K, Sercarz E, Kourilsky P. Tolerance to a self-protein involves its immunodominant but does not involve its subdominant determinants. *Proc Natl Acad Sci USA* 1992; **89**: 416–20.

3 Fedoseyeva EV, Boisgerault F, Anosova NG, Wollish WS, Arlotta P, Jensen PE, Ono SJ, Benichou G. CD4+ T cell responses to self- and mutated p53 determinants during tumorigenesis in mice. *J Immunol* 2000; **164**:5641–51.

4 McArdle SE, Rees RC, Mulcahy KA, Saba J, McIntyre CA, Murray AK. Induction of human cytotoxic T lymphocytes that preferentially recognise tumour cells bearing a conformational p53 mutant. *Cancer Immunol Immunother* 2000; **49**:417–25.

5 Theobald M, Biggs J, Hernandez J, Lustgarten J, Labadie C, Sherman LA. Tolerance to p53 by A2.1-restricted cytotoxic T lymphocytes. *J Exp Med* 1997; **185**:833–41.

6 Vierboom MP, Nijman HW, Offringa R *et al.* Tumor eradication by wild-type p53-specific cytotoxic T lymphocytes. *J Exp Med* 1997; **186**:695–704.

7 Andersen ML, Ruhwald M, Nissen MH, Buus S, Claesson MH. Self-peptides with intermediate capacity to bind and stabilize MHC class I molecules may be immunogenic. *Scand J Immunol* 2003; **57**:21–7.

8 Apostolopoulos V, Haurum JS, McKenzie IF. MUC1 peptide epitopes associated with five different H-2 class I molecules. *Eur J Immunol* 1997; **27**:2579–87.

9 Apostolopoulos V, Karanikas V, Haurum JS, McKenzie IF. Induction of HLA-A2-restricted CTLs to the mucin 1 human breast cancer antigen. *J Immunol* 1997; **159**:5211–18.

10 Apostolopoulos V, Lazoura E. Noncanonical peptides in complex with MHC class I. *Expert Rev Vaccines* 2004; **3**:151–62.

11 Apostolopoulos V, Matsoukas J, Plebanski M, Mavromoustakos T. Applications of peptide mimetics in cancer. *Curr Med Chem* 2002; **9**:411–20.

12 Apostolopoulos V, McKenzie IF, Wilson IA. Getting into the groove: unusual features of peptide binding to MHC class I molecules and implications in vaccine design. *Front Biosci* 2001; **6**:D1311–20.

13 Apostolopoulos V, Yu M, Corper AL, Li W, McKenzie IF, Teyton L, Wilson IA, Plebanski M. Crystal structure of a non-canonical high affinity peptide complexed with MHC class I. A novel use of alternative anchors. *J Mol Biol* 2002; **318**:1307–16.

14 Apostolopoulos V, Yu M, Corper AL, Teyton L, Pietersz GA, McKenzie IF, Wilson IA, Plebanski M. Crystal structure of a non-canonical low-affinity peptide complexed with MHC class I. A new approach for vaccine design. *J Mol Biol* 2002; **318**:1293–305.

15 Apostolopoulos V, Yu M, McKenzie IF, Wilson IA. Structural implications for the design of molecular vaccines. *Curr Opin Mol Ther* 2000; **2**:29–36.

16 Apostolopoulos V, Yuriev E, Ramsland PA *et al.* A glycopeptide in complex with MHC class I uses the GalNAc residue as an anchor. *Proc Natl Acad Sci USA* 2003; **100**:15029–34.

17 Lazoura E, Apostolopoulos V. Rational peptide-based vaccine design for cancer immunotherapeutic applications. *Curr Med Chem* 2005; **12**:629–39.

18 Lazoura E, Apostolopoulos V. Insights into peptide-based vaccine design for cancer immunotherapy. *Curr Med Chem* 2005; **12**:1481–94.

19 Sette A, Vitiello A, Reherman B *et al.* The relationship between class I binding affinity and immunogenicity of potential cytotoxic T cell epitopes. *J Immunol* 1994; **153**:5586–92.

20 van der Burg SH, Visseren MJ, Brandt RM, Kast WM, Melief CJ. Immunogenicity of peptides bound to MHC class I molecules depends on the MHC-peptide complex stability. *J Immunol* 1996; **156**:3308–14.

21 Rammensee H, Bachmann J, Emmerich NP, Bachor OA, Stevanovic S. SYFPEITHI. database for MHC ligands and peptide motifs. *Immunogenetics* 1999; **50**:213–19.

22 Rammensee HG. Chemistry of peptides associated with MHC class I and class II molecules. *Curr Opin Immunol* 1995; **7**:85–96.

23 Rammensee HG, Friede T, Stevanoviic S. MHC ligands and peptide motifs: first listing. *Immunogenetics* 1995; **41**:178–228.

24 Degano M, Garcia KC, Apostolopoulos V, Rudolph MG, Teyton L, Wilson IA. A functional hot spot for antigen recognition in a superagonist TCR/MHC complex. *Immunity* 2000; **12**:251–61.

25 Fremont DH, Matsumura M, Stura EA, Peterson PA, Wilson IA. Crystal structures of two viral peptides in complex with murine MHC class I H-2Kb. *Science* 1992; **257**:919–27.

26 Fremont DH, Stura EA, Matsumura M, Peterson PA, Wilson IA. Crystal structure of an H-2Kb-ovalbumin peptide complex reveals the interplay of primary and secondary anchor positions in the major histocompatibility complex binding groove. *Proc Natl Acad Sci USA* 1995; **92**:2479–83.

27 Gao L, Walter J, Travers P, Stauss H, Chain BM. Tumor-associated E6 protein of human papillomavirus type 16 contains an unusual H-2Kb-restricted cytotoxic T cell epitope. *J Immunol* 1995; **155**:5519–26.

28 Ostrov DA, Roden MM, Shi W *et al.* How H13 histocompatibility peptides differing by a single methyl group and lacking conventional MHC binding anchor motifs determine self-nonself discrimination. *J Immunol* 2002; **168**:283–9.

29 Jackson MR, Song ES, Yang Y, Peterson PA. Empty and peptide-containing conformers of class I major histocompatibility complex molecules expressed in *Drosophila melanogaster* cells. *Proc Natl Acad Sci USA* 1992; **89**:12117–21.

30 Saito Y, Peterson PA, Matsumura M. Quantitation of peptide anchor residue contributions to class I major histocompatibility complex molecule binding. *J Biol Chem* 1993; **268**:21309–17.

31 Stura EA, Matsumura M, Fremont DH, Saito Y, Peterson PA, Wilson IA. Crystallization of murine major histocompatibility complex class I H-2Kb with single peptides. *J Mol Biol* 1992; **228**:975–82.

32 Matsumura M, Saito Y, Jackson MR, Song ES, Peterson PA. *In vitro* peptide binding to soluble empty class I major histocompatibility complex molecules isolated from transfected *Drosophila melanogaster* cells. *J Biol Chem* 1992; **267**:23589–95.

33 Apostolopoulos V, Pouniotis DS, van Maanen PJ *et al.* Delivery of tumor associated antigens to antigen presenting cells using penetratin induces potent immune responses. Vaccine 2006; **24**:3191–202.

34 Pouniotis DS, Apostolopoulos V, Pietersz GA. Penetratin tandemly linked to a CTL peptide induces anti-tumor T cell responses via a cross-presentation pathway. *Immunol* 2006; **117**: 329–39.

35 Pouniotis DS, Proudfoot O, Bogdanoska V, Apostolopoulos V, Fifis T, Plebanski M. Dendritic cells induce immunity and long-lasting protection against blood-stage malaria despite an *in vitro* parasite-induced maturation defect. *Infect Immun* 2004; **72**:5331–9.

36 Otwinowski Z, Minor W. Processing of X-ray diffraction data collected in oscillation mode. *Meth Enzymol* 1997; **276**:307–17.

37 Roussel A, Cambillau C. *TURBO-FRODO molecular graphics program*. Mountain View, CA: Silicon Graphics Partner Directory, Silicon Graphics, 1989: 77–87.

38 Brunger AT, Adams PD, Clore GM *et al.* Crystallography and NMR system: a new software suite for macromolecular structure determination. *Acta Crystallogr D Biol Crystallogr* 1998; **54** (5):905–21.

39 Laskowski RA, Moss DS, Thornton JM. Main-chain bond lengths and bond angles in protein structures. *J Mol Biol* 1993; **231**:1049–67.

40 Gilbert SC, Plebanski M, Harris SJ, Allsopp CE, Thomas R, Layton GT, Hill AV. A protein particle vaccine containing multiple malaria epitopes. *Nat Biotechnol* 1997; **15**:1280–4.

41 Lee EA, Palmer DR, Flanagan KL *et al.* Induction of T helper type 1 and 2 responses to 19-kilodalton merozoite surface protein 1 in vaccinated healthy volunteers and adults naturally exposed to malaria. *Infect Immun* 2002; **70**:1417–21.

42 Plebanski M, Burtles SS. *In vitro* primary responses of human T cells to soluble protein antigens. *J Immunol Meth* 1994; **170**:15–25.

43 Plebanski M, Flanagan KL, Lee EA *et al.* Interleukin 10-mediated immunosuppression by a variant CD4 T cell epitope of *Plasmodium falciparum*. *Immunity* 1999; **10**:651–60.

44 Plebanski M, Gilbert SC, Schneider J *et al.* Protection from *Plasmodium berghei* infection by priming and boosting T cells to a single class I-restricted epitope with recombinant carriers suitable for human use. *Eur J Immunol* 1998; **28**:4345–55.

45 Pietersz GA, Li W, Popovski V, Caruana JA, Apostolopoulos V, McKenzie IF. Parameters for using mannan-MUC1 fusion protein to induce cellular immunity. *Cancer Immunol Immunother* 1998; **45**:321–6.

46 Jager E, Jager D, Knuth A. Clinical cancer vaccine trials. *Curr Opin Immunol* 2002; **14**:178–82.

47 Gross DA, Graff-Dubois S, Opolon P *et al.* High vaccination efficiency of low-affinity epitopes in antitumor immunotherapy. *J Clin Invest* 2004; **113**:425–33.

48 Bredenbeck A, Losch FO, Sharav T *et al.* Identification of non-canonical melanoma-associated T cell epitopes for cancer immunotherapy. *J Immunol* 2005; **174**:6716–24.

49 Tourdot S, Scardino A, Saloustrou E, Gross DA, Pascolo S, Cordopatis P, Lemonnier FA, Kosmatopoulos K. A general strategy to enhance immunogenicity of low-affinity HLA-A2.1-associated peptides: implication in the identification of cryptic tumor epitopes. *Eur J Immunol* 2000; **30**:3411–21.

50 Tirosh B, el-Shami K, Vaisman N *et al.* Immunogenicity of H-2Kb-low affinity, high affinity, and covalently-bound peptides in anti-tumor vaccination. *Immunol Lett* 1999; **70**:21–8.